Volume 15, Issue 3, 152533 (1-15)

Iranian Journal of Catalysis (IJC)

https://doi.org/10.57647/j.ijc.2025.1503.33

Efficient and greener method synthesis of pyrano[2, 3-c]pyrazole derivatives catalyzed by Fe_3O_4@L-Cys-SH as reusable catalyst

Raju Shekhanavar, Santosh Y. Khatavi, Kantharaju Kamanna*

Department of Chemistry, Rani Channamma University, Belagavi, P-B, NH-4-591156, Karnataka, India.

***Corresponding author:** kk@rcub.ac.in

Original Research

Received:
4 March 2025
Revised:
16 May 2025
Accepted:
6 June 2025
Published online:
1 July 2025
Published in issue:
30 September 2025

Abstract:

The present work describes the eco-friendly preparation of magnetic nanoparticles Fe_3O_4 (MNPs), and further functionalized with L-Cysteine amino acid. Various analytical and spectroscopic techniques used for the characterization of prepared MNPs and its functionalized materials. Further demonstrated utility of this functionalized MNPs for four component one-pot synthesis of pyrano[2, 3-c]pyrazole derivatives. The synthetic approach outlined is rapid, eco-friendly, and allows for the simple isolation of the product. After recrystallization of the crude product gave a chromatographically pure product, this method found an inexpensive and recyclable catalyst, which was achieved up to four cycles for the synthesis of bioactive heterocycles. The synthesized derivatives were characterized using FT-IR, ^{1}H- & ^{13}C-NMR, and LC-MS. Additionally, some of the selected derivatives showed moderate antioxidant activity (5a, 5 h, 5i, 5j, 5k, 5n, 5p, and 5q) against a reference.

Keywords: Antioxidant; Eco-friendly; Functionalized; Pyrano[2,3-c]pyrazole; Recyclable

1. Introduction

In recent days, bond-formation reaction has effectively paved the way for the construction of diverse molecular architecture in organic synthesis, combinatorial, and medicinal chemistry [1]. One of the routes more likely to be considered is Multi-Component Reactions (MCRs), which construct complex molecules in one pot, sparking the attention of researchers. This method has various advantages like high atom economy, eco-friendliness, single-step, and high yield isolation [2]. Due to these benefits drawn from the MCRs, they are easily amenable to the efficient generation of diverse libraries of valuable bioactive heterocycles and metal chelation agents [3]. This reaction is called one-pot, where the reactants of three or more undergo a reaction to form multiple bonds, making and breaking, and also do not lead to any side reactions [4]. MCRs, especially in aqueous medium, have proven to be a valuable synthetic route for the synthesis of a wide range of different biologically active compounds [5]. In the present environmental concern, chemists prefer green solvent media for the synthetic methods, and require common miscibility of the substrates for homogeneous heat transfer between the reactants in MCRs [6]. Water, the safest and most abundant in the universe, is referred to as a benign universal solvent [7]. The design and development of new MCRs using environment-friendly methods remains challenging and is a cutting-edge area in the green chemistry protocol [8]. Historically, the approach to discovering drugs hasn't changed much, because these drugs were discovered by extraction from herbal remedies or by serendipity [9]. However, in recent years, advancements in drug discovery have involved lead identification by computational methods with more accuracy, synthesis made by efficient methods, and screening becoming robust [10, 11]. Heterocycles are the largest form of organic molecules and have contributed immensely to the biological, pharmaceutical, and indeed to any developed human

society. A vast number of heterocycles discovered by nature and synthetically made are shown to be very good drug candidates currently used in the treatment [12]. Among various heterocycle skeletons, pyrazole is an important class of five-membered heterocycles attracting attention in several active pharmaceutical ingredients, photographic couplers, chelating agents, and agrochemicals [13]. The pyrazole scaffold has evidenced potential pharmacological application, and several FDA approved drugs related to its scaffold includes Celecoxib [14], Phenylbutazone [15], Ramifenazone [16], Antipyrine [17], Lonazolac [18] and Zaleplon [19] are available marketed drugs (Fig. 1).

Various ring-fused nitrogen and oxygen-containing heterocycles like pyranopyrazole derivatives represent an important group of natural and synthetic heterocyclic derivatives [20]. The pyranopyrazole moiety exhibited pyrano[2,3-c]pyrazole (i), pyrano[3,2-c]pyrazole (ii), pyrano[3,4-c]pyrazole (iii), and pyrano[4,3-c]pyrazole (iv) as four isomeric forms presented in Fig. 2 [21], but the pyrano[2,3-c]pyrazole skeleton has been most extensively investigated, and showed biological compatibility [22]. This pyrano pyrazole skeleton containing molecules showed anticancer, anti-inflammatory, antimicrobial, fungicidal, insecticidal, molluscicidal, analgesic, antiviral, and antidepressant activities [23].

Recent years have also demonstrated DNA-binding capacity and cholinesterase inhibition [24] (Fig. 3), and substantial studies have been described for the synthesis of heterocyclic motifs based on the different approaches [25]. Numerous reported synthetic routes for the pyrano[2, 3-c]pyrazoles derivatives via the condensation reaction of hydrazine hydrate (**1**), malononitrile (**2**), ethyl acetoacetate (**3**), and aryl aldehyde in the presence of catalysts such as $ZnFe_2O_4$ [26], $CuFe_2O_4$ [27], PMO/Chit/Fe_3O_4 [28], CPs-COM-NPs [29], $Y_3Fe_5O_{12}$ [30], Fe_3O_4-CNT-ln [31], Biochar/Fe_3O_4@TiO_2 [32], Zirconium MNPs [33], Agar supported ZnS/$CuFe_2O_4$ [34], CuNPs [35], Carr-Mett-MNPs [36], MNPs@DABCO$^+$Cl$^-$ [37], Glu@Fe_3O_4 [38], Fe_3O_4@cellulose [39], Fe_3O_4@guanidine [40], Fe_3O_4@Cellulose@SO_3H [41], Fe_3O_4@Ag-B-CD [42], Fe_3O_4@L-Arg [43], Fe_3O_4@GO@Melamine-ZnO [44], SCMNPs@Uridine [45] and recently various modified NPs catalysts employed for various MCRs PVA@SO_3H [46], Fe_3O_4@SiO_2@KIT-6, MMNPs [47], Fe_3O_4@SiO_2@KIT-6-NH_2@schiff [48], Fe_3O_4@SiO_2@vanillin@thioglycolic acid [49], [PVP-SO_3H] HSO_4 [50], and $CoNiFe_2O_4$ [51]. In this paper, a one-pot four-component reaction of hydrazine hydrate, malononitrile, ethyl acetoacetate, and benzaldehyde was demonstrated, giving the title product catalyzed by Fe_3O_4@L-Cys in EtOH under a custom-made microwave oven.

2. Materials and methods

2.1 Preparation of WELFSA

The lemon peel was obtained from a local fruit market in Belagavi, India. The outer shell is removed and washed with tap water to remove physical impurities on the surface. Then dried the peel in the shade, and directly burnt it on a Bunsen flame to get lemon peel ash. 10 g of this ash was taken, dispersed in 100 mL double-distilled water, and stirred for **one** hour at room temperature. The mixture was filtered, the light brown-colour filtrate named Water Extract of Lemon Fruit Shell Ash (WELFSA) and stored till next use.

2.2 Preparation of Fe_3O_4 using WELFSA

The equal weight 3 g each $FeSO_4 \cdot 7H_2O$ and $FeCl_3 \cdot 6H_2O$ dissolved in 50 mL of double-distilled water (dd water) taken in a 100 mL beaker, and then 10 mL of the above-

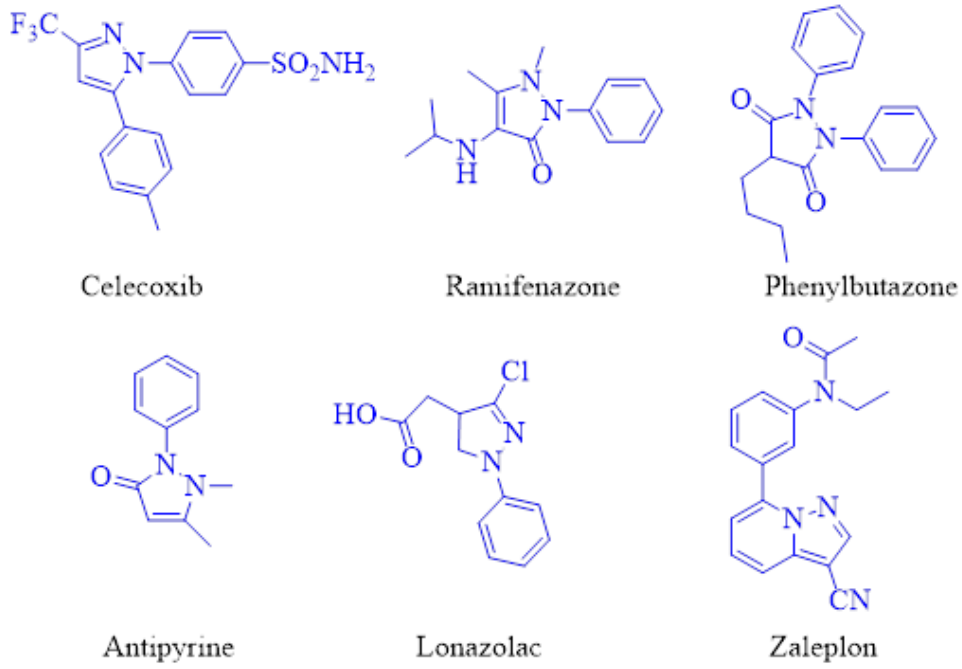

Figure 1. The pyrazole skeleton contains some drug molecules.

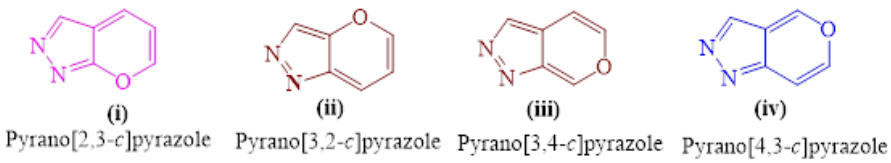

Figure 2. Pyrano pyrazole isomers.

prepared WELFSA was added to it. The suspension was heated to 85 °C for approximately 45 min while stirring, and then allowed to cool to room temperature. NaOH solution was added drop-wise until a black precipitate appeared. The black precipitate was pulled out using a strong magnet and washed 2 – 3 times with dd water and EtOH. The residue obtained was dried and calcinated at 400 °C for about four hours in a muffle furnace, and stored in a desiccator in an air-tight container till further use.

2.3 Preparation of Fe_3O_4@L-Cys

The above-prepared Fe_3O_4 MNPs (2 g) and L-Cys (1.5 g) were stirred in 50 mL methanol: water (1:1) at room temperature for 24 h at 1800 rpm. The isolation of the Fe_3O_4@L-Cys MNPs was simply magnetic decantation, and washed several times with dd water and methanol, and then dried in a vacuum at 70 °C for two hours.

2.4 General procedure for the synthesis of pyrano[2, 3-c]pyrazole derivatives

Taken hydrazine hydrate (1) (50.04 g/mol), malononitrile (2) (66.06 g/mol), ethyl acetoacetate (3) (130.14 g/mol), and benzaldehyde (4) (106.05 g/mol) in the presence of Fe_3O_4@L-Cys (25 mg) catalyst in EtOH (2 mL) at a specified time MWI at 300 W power. The reaction was monitored by TLC mobile phase (ethyl acetate: hexane 0.5:9.5). After the reaction, the reaction mixture was quenched with 15 mL of hot ethanol, hold the catalyst by an external magnet, decanted ethanol, concentrated and recrystallized at room temperature gave title products (5) in good yields with no further purification required. The new compound's structure is established based on the FT-IR, ^{1}H- & ^{13}C-NMR, and mass spectrometry techniques. The physical and spectroscopic data were found to be matched with the proposed structure, and are in good agreement with the literature.

2.5 Antioxidant activity

DPPH radical scavenging assays were performed to evaluate the in vitro antioxidant activity of the selected pyrano[2,3-c]pyrazole derivatives. A sample solution was prepared in DMSO and transferred separately into test tubes at different concentrations of samples, 200, 400, 600, 800, 1000 μg/μL, and reference. To each of these tubes, 5 mL of 0.1 mM ethanolic solution of DPPH was added, and mixed vigorously. All test tubes are incubated in the dark room for about 30 minutes. The absorbance of the sample was taken at 517 nm, and ascorbic acid was used as a standard.

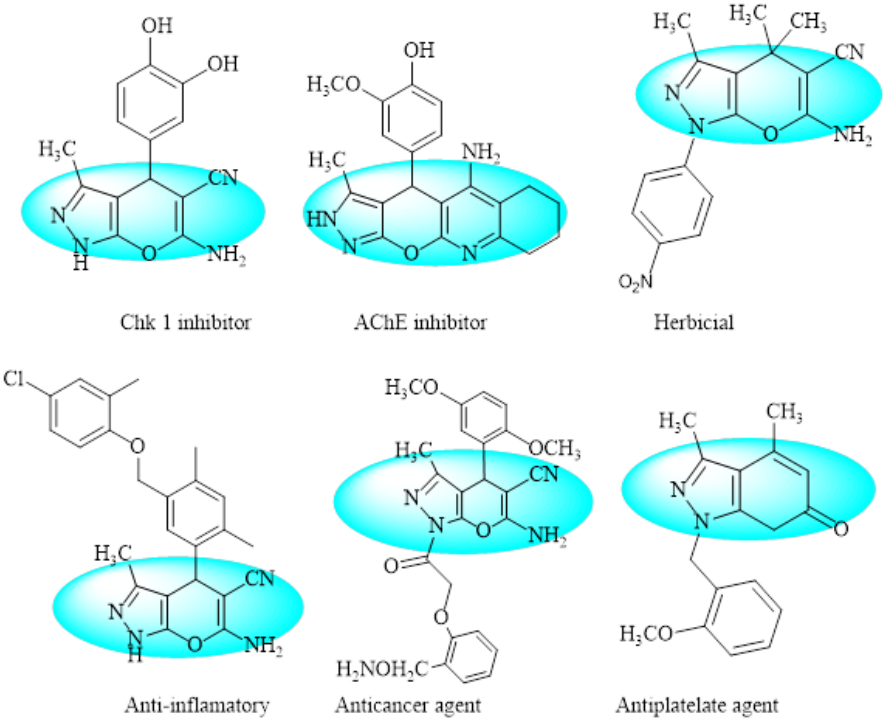

Figure 3. Biologically active pyrano pyrazole.

It is reduced when an antioxidant molecule is present, and the result is a decolourisation in ethanol solution. In other words, the reduced DPPH radicals are directly proportional to oxidized antioxidants. The formula below was used to assess radical scavenging

$$\text{Inhibition ratio } \% = \frac{\text{controlled OD} - \text{sample OD}}{\text{controlled OD}} \times 100$$

2.6 Spectral data of selected compounds

2.6.1 6-Amino-3-methyl-4-phenyl-1,4-dihydropyrano[2,3-c]pyrazole-5-carbonitrile (5a)

White solid; m.p. 198 °C; FT-IR (cm^{-1}): 3731.82, 3552.51 (NH), 3162.68 (C-H, sp^2), 2916.66, 2032.66, (CH_2); ^{1}H-NMR δ(ppm): 1.83 (s, 2H, NH), 4.54 (s, 1H, CH), 6.83 (s, 2H, CH_3), 7.17 (t, J = 6.9Hz, 2H, Ar-H), 7.27 (t, J = 6.3Hz, 1H, Ar-H), 7.43 (t, J = 7.3 Hz, 2H, Ar-H), 8.00 (s, 1H, NH) ppm; ^{13}C NMR δ(ppm): 10.18 (CH_3-C), 36.34, 39.48, 40.112, 56.39 (C-O-C), 97.01, 120.93 (C=C), 129.30 (CH-C), 136.22 (C-C), 146.85, 155.108, 161.60 (C-N); LC-MS: m/z (Obs): 252.10 $[M+H]^+$, $C_{14}H_{12}N_4O$ (Calcd.): 252.28 Da.

2.6.2 6-Amino-3-methyl-4-(4-nitrophenyl)-1,4-dihydropyrano[2,3-c]pyrazole-5-carbonitrile (5g)

Light orange; FT-IR (cm^{-1}): 3475.79, 3280.76 (NH_2), 3198.20 (C-H, sp^2), 1680.34, 1591.93, 1490.59, 1345.23; ^{13}C NMR δ (ppm): 120.93 (C-C), 124.35 (CH-C), 125.78 (CH-N), 129.30 (CH-C), 136.41 (C-C), 146.85 (C-N), 152.52, 161.56 (C-O); ^{1}H-NMR δ (ppm): 1.78 (s, 3H, CH_3), 5.20 (s, 1H, CH), 7.08 (s, 1H, Ar-H), 7.63-7.67 (m, 1H, Ar-H), 7.80 – 7.83 (m, 1H, Ar-H), 7.95 – 7.97 (m, 1H, Ar-H), 8.05 – 8.07 (m, 1H, Ar-H), 8.39 (s, 1H, Ar-H), 12.20 (s, 1H, NH); LC-MS: m/z (Calcd.) = 297.41 Da; m/z (Obs) = 298.42 Da.

2.6.3 6-Amino-4-(2-chloroquinolin-3-yl)-3-methyl-1,4-dihydropyrano[2,3-c]pyrazole-5-carbonitrile (5j)

Light yellow; FT-IR (cm^{-1}): 3719.69, 3405.60 (NH_2), 3162.10 (C-H, sp^2), 1649.34, 1585.96, 1450.27, 1326.49, 1160.16, 1026.42, 930.43, 829.92; ^{13}C NMR δ (ppm): 165.72, 157.94 (C-Cl), 145.63 (C-C), 141.87, 140.79 (C-C), 137.16 (CH-C), 134.35, 130.64 (CH-C), 128.05 (CH-C), 126.02 (C-C), 116.99 (C-CN) ppm; ^{1}H-NMR δ(ppm): 1.80 (s, 3H, CH_3), 4.83(s, 1H, CH), 7.05 (s, 1H, Ar-H), 7.45 – 7.48 (m, 3H, Ar-H), 7.97 – 8.87 (m, 3H, Ar-H), 12.22 (s, 1H, NH); LC-MS: m/z (Calcd.) = 337.14 Da; m/z (Obs.) = 338.59 Da.

3. Results and discussion

3.1 Preparation and characterization of catalysts (Fe_3O_4@L-Cys)

The catalyst core shell (Fe_3O_4) is prepared using an agro-waste extract medium using a previously reported procedure [52]. The method developed was a chemical-free synthesis to give free-flowing magnetic Fe_3O_4. Further, its outer surface was modified with natural amino acid L-Cysteine, giving Fe_3O_4@L-Cys (Scheme 1).

The prepared catalyst was subjected to various spectroscopic techniques. Firstly, the Raman spectrum was collected for Fe_3O_4@L-Cys, and characteristic peaks were observed at 389 and 425 cm^{-1} for the iron oxide as shown in Fig. 4. Also, the Raman spectrum was collected for the reused catalysts after the fifth cycle, and showed a similar pattern of peaks with low intensity to fresh catalysts (Fig. S17). In the XRD pattern, the surface of the MNPs modified with Cys indicates a crystalline nature, and other peaks become more pronounced at 2θ values.

Due to the -SH group present on the top of the substrate at 18.85°. To identify the presence of characteristic 2θ values 30.22°, 35.46°, 43.17°, 53.66°, 57.34°, and 63.06° for the Fe_3O_4. The 2θ values corresponding to the Miller indices of the cubic iron oxide phase (inverse spinel ferrite, JCPDS file no.19-0629) [53]. Therefore, the pattern of the XRD diffractogram revealed the deposition of the Cys on the surface of Fe_3O_4 (Fig. 5), and also collected reused XRD of the catalysts after the fifth cycle showed no change in the pattern of the spectrum (Fig. S18).

Further, dried catalyst was loaded on carbon tape on FE-SEM to record the surface morphology and presence of the elements in the prepared catalysts. The FE-SEM image shows the development of small crystalline structures (Fig. 6a) and functionalization of the core shell (Fig. 6b). The tiny grooves are located on the surface of the Fe_3O_4, and also collected FE-SEM image of the reused catalysts, but the morphology showed fewer densities of the functionalized L-Cys compared to the fresh sample image, as shown in Fig. S19. Additionally, the elemental mapping evidence

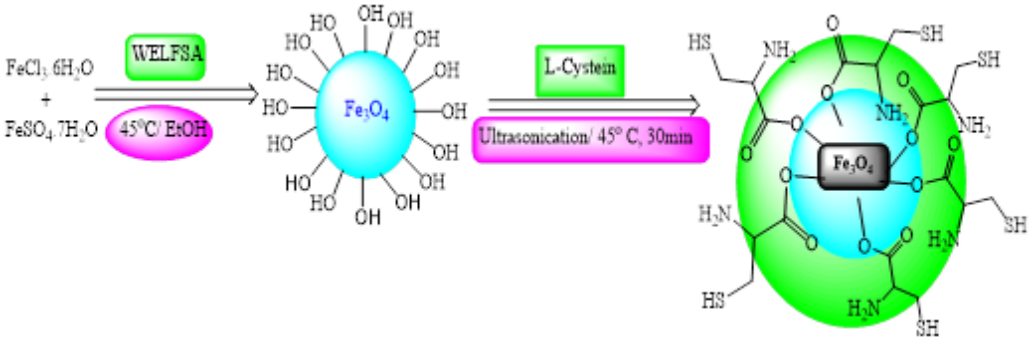

Scheme 1. Preparation of Fe_3O_4@L-Cys.

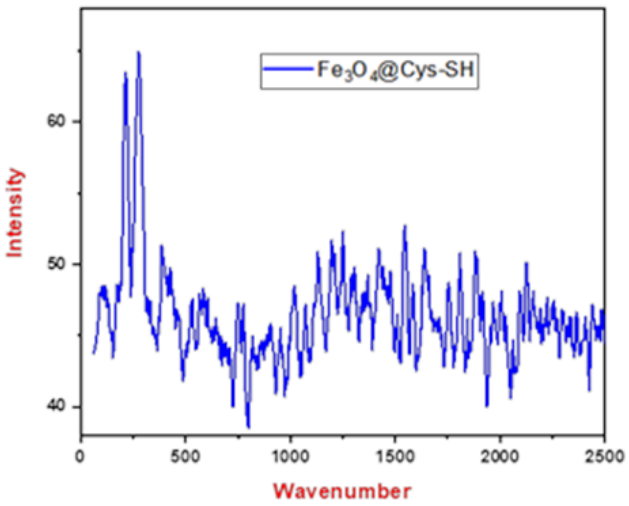

Figure 4. Raman spectra of Fe_3O_4@L-Cys.

shows the presence of elements Fe, O, N, and S (Fig. 6c), and reused elemental mapping also revealed the presence of the elements Fig. S20. Furthermore, the EDS spectra peaks at 2.09 keV attributed to the S-peak, and a prominent peak around 0.5 keV corresponds to the N peak, and a peak at 6.4 eV due to the presence of Fe (Fig. 7), and a similar pattern of elemental mapping was noticed for the reused catalysts (Fig. S21).

The Vibrating Sample Magnetometer (VSM) was used to investigate the magnetic behavior of the Fe_3O_4 and Fe_3O_4@L-Cys samples in the 15 KG to -15 KG applied field at room temperature (Fig. 8), and from its exposure to ferromagnetic properties. Specifically, the M-H plot given in Table 1 was used to approximate the converse magnetization properties such as magnetic saturation (**Ms**), coercivity (**Hc**), and remnant magnetization (**Mr**). In Table 1, pure Fe_3O_4 shows a high **Ms** value, but after decoration with L-Cysteine, the **Ms** value decreases significantly up to 40.17 emu/gm. This implies that the magnetic saturation of the dopant is diminished as the coercivity rises from 5.04 G to 6.85 G for higher dopants, which indicates that the strong magnetism slowly decreases with the dopants. The magnetic properties studied by VSM at rt ranging from applied field of 1 T to +1 T. The values for magnetic properties such as magnetic saturation (**Ms**), remnant magnetization (**Mr**), coercivity (**Hc**), and magnetic susceptibility (**X**) were calculated and listed in Table 1. The **Ms** drops prominently from 36.11 to 1.63 emu/g, such a typical nature was observed because the L-Cys does not have a magnetic nature, and reused iron oxide with L-Cys magnetic behavior was also collected and showed a similar pattern to the fresh sample, and is appended in Fig. S22.

In FT-IR, the presence of a strong absorption peak at 600 cm^{-1} is due to the presence of iron oxide of the Fe-O stretching vibration of the tetrahedral and C=C site of the spinel structure. The strong absorption band at 1602 cm^{-1} is due to the OH bending of physically held water molecules. The strong peak at 3300 cm^{-1} is due to the O-H stretching of water adsorbed on the surface of Fe_3O_4. The weak bands at 845 and 1032 cm^{-1} are due to the C-O stretching of the surface carbon layer. The prominent peak at 3351 cm^{-1} is due to the surface -OH stretching of the -SH (Fig. 9). The reused catalysts' FT-IR spectra also resemble the fresh catalyst's spectrum and are appended in Fig. S23.

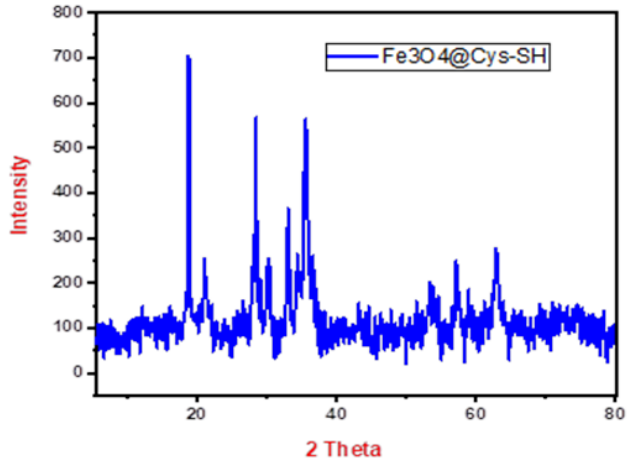

Figure 5. XRD profile of Fe_3O_4@L-Cys.

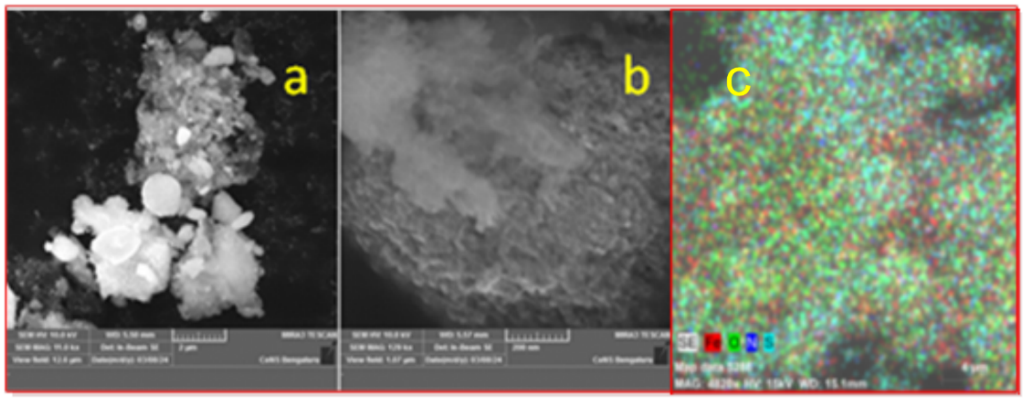

Figure 6. FE-SEM image of the core shell and fabricated (**a** & **b**), and elemental mapping (**c**).

Further, the thermal stability of the synthesized Fe_3O_4@L-Cys catalyst was investigated by thermal gravimetric analysis (TGA), which helped to evaluate the stability of the catalysts. The TGA curve in Fig. 10 demonstrates 7% initial weight loss at temperatures lower than 100 °C, and weight loss from 100 – 185 °C is related to evaporation of the surface water. TGA analysis was used for the determination of the weight changes of the organic functional groups of the Fe_3O_4@L-Cys heating, and degradation of the organic groups was not observed in the range of 100 to 600 °C. Since the catalyst weight loss did not occur except above 600 °C, this implies its high thermal stability, which is advantageous as many organic compounds may be synthesized at higher temperatures (Fig. 10).

The Zeta potential was used to understand the surface charge of the MNPs and predict their long-term dispersion stability. According to previous reports, nanoparticles with zeta potential values between +26 and −26 mV are usually very stable. As shown in Fig. 11, the zeta potential was scanned, and the value of dispersed catalyst in distilled water and in the absence of any electrolyte was found to be 25.1 mV.

The nitrogen adsorption-desorption isotherms of iron oxide functionalized L-Cys are shown in Fig. 12. The catalytic system shows a type-IV isotherm, which, according to the IUPAC classification, confirms the catalysts have a mesoporous structure. According to the Brunauer-Emmett-Teller (BET) technique, the surface functionalized L-Cys is 50.32 m^2/g. The obtained BET results, such as surface area, total pore volume, average pore diameter, and average pore width, are depicted in Table 2.

To explore the application of the prepared heterogeneous catalysts Fe_3O_4@L-Cys, herein demonstrated for the synthesis of pyrano[2,3-c]pyrazole derivatives based upon the model reaction of hydrazine hydrate (1), malononitrile (2), ethyl acetoacetate (3), and benzaldehyde (4), gave the title product (5). The reaction was catalyzed by Fe_3O_4@L-Cys (25 mg) in EtOH solvent under custom-made MWI of 6 min. After the reaction completion, the reaction was monitored by TLC. After reaction completion, hot ethanol was added (10 mL), and an external strong magnetic field was used to separate the catalyst used, and then the product was quickly isolated after recrystallization (Scheme 2).

3.2 Optimization of the reaction

To achieve the best condition required for the reaction, a model reaction was performed with different amounts of the catalyst starting from 0, 5, 20, 25, and 30 mg of the catalyst under MWI at 300 W power, and the isolated products are compiled in Table 3. The experimental data showed that with an increase of 5 – 25 mg quantity of catalyst, a gradual increase in the product yield was observed (entries 2 – 5, Table 3). But, if the amount of the catalyst increased to 30

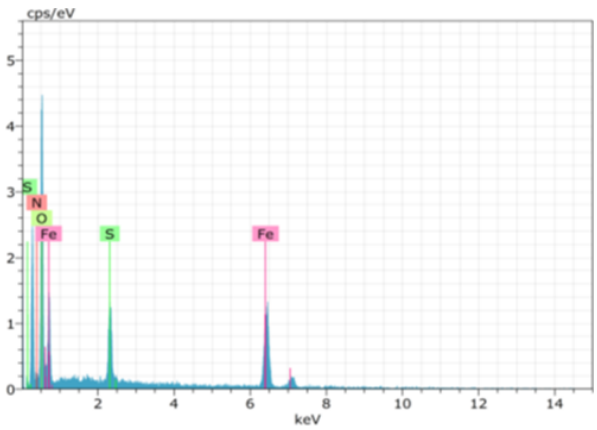

Figure 7. Elemental composition of iron-oxide@L-Cys.

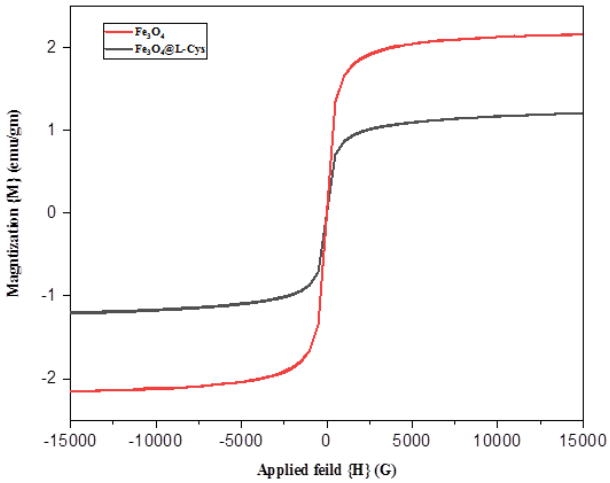

Figure 8. VSM Profile of Fe3O4 and Fe_3O_4@L-Cys.

Table 1. Magnetic saturation (**Ms**), remanent magnetization (**Mr**), coercivity (**Hc**), and magnetic susceptibility (**X**) data.

Sample	Ms. (emu/g)	Mr. (emu/g)	Hc. (Oe)	X. (emu/g.Oe)
Fe_3O_4	40.17	0.43	357.05	0.00518
Fe_3O_4@L-cys	5.25	0.22	354.52	0.000577

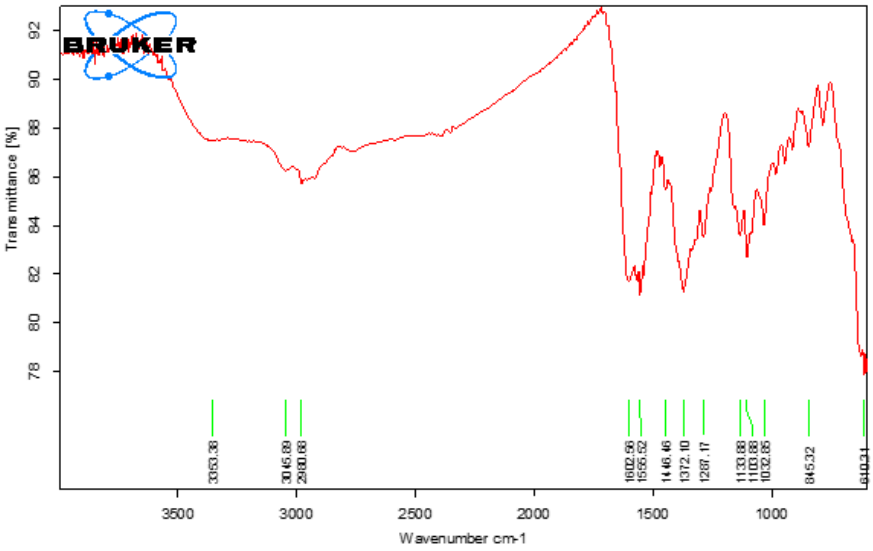

Figure 9. FT-IR Spectra of Fe_3O_4@L-Cys.

mg, the product yield isolation remained unchanged in 6 min MWI. In another experiment, where no catalyst (entry 1, Table 3), no product formation was observed in TLC. This reaction revealed that the reaction required a catalyst for the product formation. The optimization reaction showed that, for a 1 mmol scale reaction, high product isolation was observed in 25 mg of the catalyst used in 6 min MWI (entry 5, Table 3). Moreover, for microwave power 300 W, a quite suitable output power for this reaction acceleration was found, and high product yield isolation was achieved. To optimize the MW power required for the model reaction, a series of reactions with varying MW power starting from 100, 180, 300, and 450 W were examined. The product isolation was noticed at its highest in 300 W power in 6 min irradiation time (entry 6, Table 4), and a decrease in MW power (180 and 100 W) led to longer reaction times with incomplete and lower product yield isolation (entries 4 & 5, Table 4). However, in the case of high MW power of 450 W, low yield product isolation may be due to excess heating and reactant loss (entry 7, Table 4). In addition, it is investigated in a model reaction different reaction techniques, such as grinding, ultrasound, and rt stirring methods. These three methods required longer reaction times and provided very poor product isolation (entries 1 – 3, Table 4).

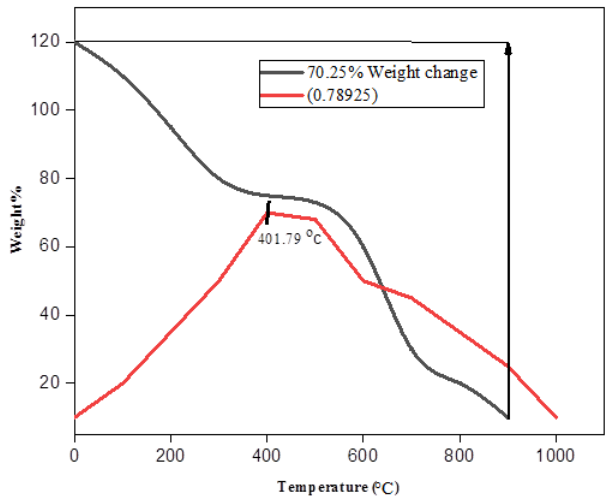

Figure 10. The TGA-DTG image of Fe_3O_4@L-Cys.

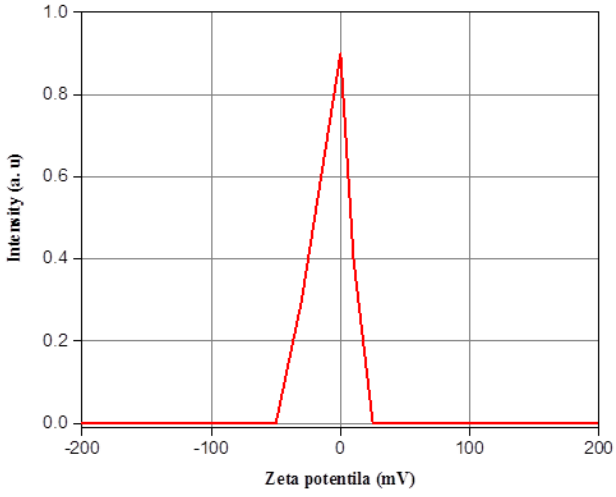

Figure 11. The Zeta potential image of Fe_3O_4@L-Cys.

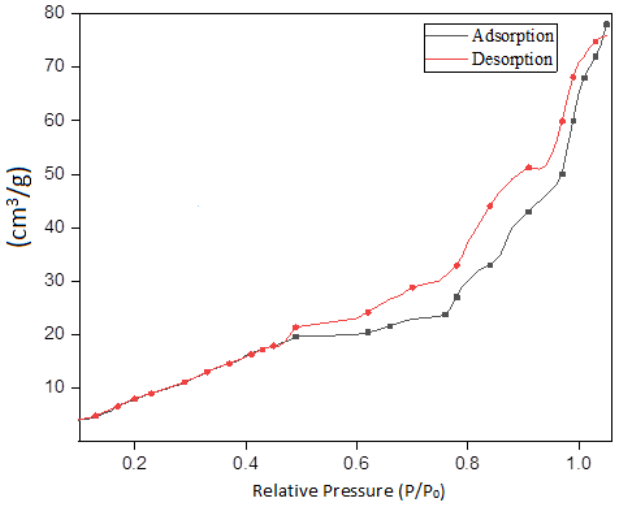

Figure 12. The nitrogen adsorption & desorption isotherms of Fe_3O_4@L-Cys.

To check the diversity and tolerance of the developed protocol on the substrate compatibility with different substituents present on the aromatic aldehyde containing an electron-withdrawing group (EWG) and an electron-donating group (EDG) was investigated. The substituent of either EWG or EDG groups present on the aryl aldehyde did not show any measurable effect on the rate of the reaction, and the isolation of the product yield (Table 5). However, it is noticed that, there is a reduction in the aryl aldehyde reactivity due to steric hindrance in the vicinity of the reactive site, the reactivity of the aldehyde-bearing electron-donating groups (OCH_3, CH_3) & were significantly high reaction rate than electron-withdrawing groups (Cl, F, NO_2, CN) distributed around the aromatic aldehyde.

3.3 Comparison of the present approach with the literature reported

We compared the present method with selected reported methods used for pyrano[2, 3-c]pyrazole synthesis (Table 6). To evaluate these heterogeneous catalysts reported, they are expensive and a hyper-sensitized reaction (entries no. 1, 2, 3, 6, and 11). Many of the techniques that are employed are costly and use dangerous solvents (Table 6, entries 4, 5, 7, 9, 10), time-consuming, and give low yield isolation of the product. All these disadvantages motivated us to come up with economic, eco-friendly, and recyclable catalysts for the synthesis of pyrano[2,3-c]pyrazole scaffolds.

3.4 Reusability of catalysts

A model reaction was carried out for the synthesis of pyrano[2, 3-c]pyrazoles from benzaldehyde, hydrazine hydrate, ethyl acetoacetate, and ethylcyanoacetete in the presence of the catalyst under optimized reaction conditions. The completion of the reaction was followed by the addition of hot ethanol into the reaction mixture and the separation of the catalyst using a strong magnet. The catalyst was washed 2 times with 50 mL distilled water, and once with 10 mL EtOH, dried under vacuum at 80 °C for 5 h, and then used in the consecutive cycles. The catalyst activity was monitored up to four cycles, and it was noticed without significant loss of its catalyst efficiency, though a comparatively low yield was isolated in the fifth cycle (Fig. 13).
Turnover frequency (TOF) and turnover number (TON) values for the catalysts and recycled for up to 5 run calculated. Both the numbers decreases in each cycle due to loss of the active site or poisoning. The TOF and TON values were summarized in Table 7.

3.5 A plausible mechanism

Exact mechanistic pathway via a heterogeneous catalyst has not been explicitly elucidated, but it is assumed to have an intuitive mechanism compared to the utilization of the organic or inorganic base replaced by a heterogeneous catalyst (Fig. S16). In the first step, one of the active hydrogen is abstracted from malononitrile (2) gave carbanion formation (2a), it is nucleophilic, and attacks the carbonyl carbon of the arylaldehyde (4), loss of water molecule and generates an arylidene malononitrile (4a). Alternatively, 3-methyl-5-pyrazolone (1a) made from ethyl acetoacetate (3) and hydrazine hydrate (1) and its enolic isomer (1b) undergoes

Table 2. Surface area, average pore width, volume & diameter of Fe_3O_4@L-Cys.

BET surface area m^2/g	Langmuir surface area	Total pore volume cm^3/g	Average pore diameter A	Average pore width A
50.32	142.11	0.10	75.25	22.08

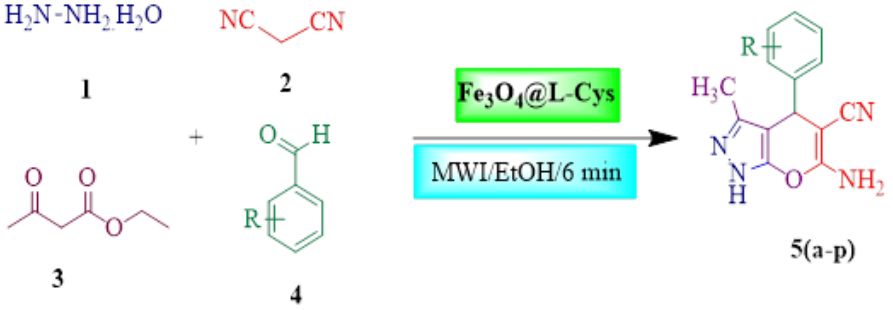

Scheme 2. Pyrano[2, 3-c]pyrazole synthesis.

Table 3. The quantity of the catalyst required in a model reaction (1 mmole).

Entry	Quantity of catalyst (mg)	Time (min)	Yield%
1	0	6	Nil
2	5	6	28
3	10	6	36
4	20	6	70
5	25	6	93
6	30	6	90

Table 4. Rate of reaction vs power and optimization.

Entry	Methods	Power (W)	Time (min)	Yield (%)
1	Grindstone	-	30	48
2	Ultrasound	-	75	70
3	rt	-	80	62
4	MWI	100	9	60
5	MWI	180	7	78
6	MWI	300	6	94
7	MWI	450	7	90

Table 5. Pyrano[2, 3-c]pyrazoles yield, structure, and physical data.

Entry	Aldehyde	Product	TON/TOF	Yield (%)	m.p. (°C) Obs./Lit.	Ref.
1	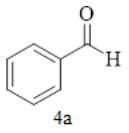 4a	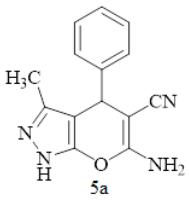 5a	129.4/10.1	92	195/ 197 – 198	[54]
2	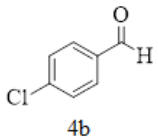 4b	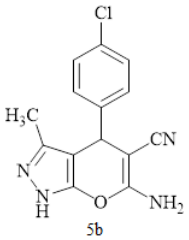 5b	128.1/9.6	86	234/ 233 – 235	[54]
3	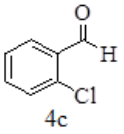 4c	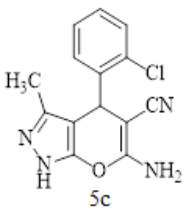 5c	127.3/9.1	90	216/ 214 – 216	[54]

Continued of Table 5.

Entry	Aldehyde	Product	TON/TOF	Yield (%)	m.p. (°C) Obs./Lit.	Ref.
4	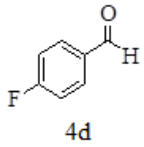 4d	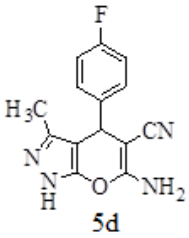 5d	126.6/8.7	85	170/ 168 – 170	[54]
5	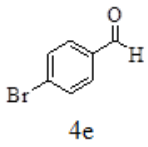 4e	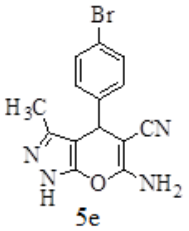 5e	124.56/8.1	88	181/ 180 – 182	[54]
6	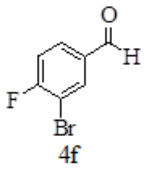 4f	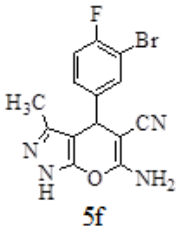 5f	130.5/7.5	86	223/ 224 – 226	[54]
7	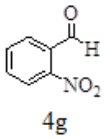 4g	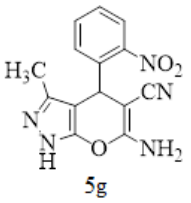 5g	132.5/7.0	84	262 – 263 New	[54]
8	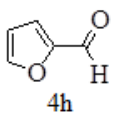 4h	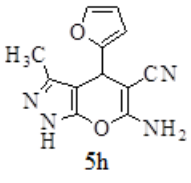 5h	130.5/6.8	88	215/ 215 – 217	[54]

Continued of Table 5.

Entry	Aldehyde	Product	TON/TOF	Yield (%)	m.p. (°C) Obs./Lit.	Ref.
9	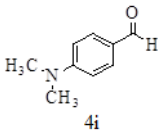 4i	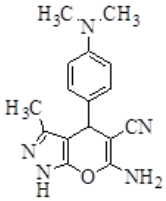 5i	131.6/7.9	86	164/ 162 – 164	[54]
10	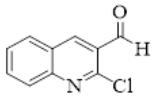 4j	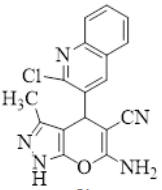 5j	135.7/8.1	91	215 – 216 New	[54]
11	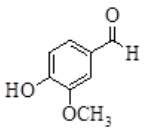 4k	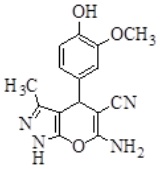 5k	130.6/7.9	88	234/ 234 – 236	[54]
12	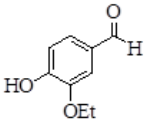 4l	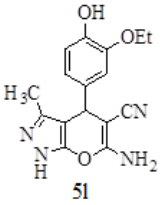 5l	126.5/7.5	92	193/ 192 – 194	[54]
13	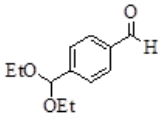 4m	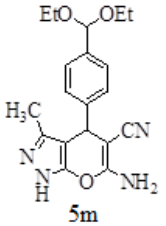 5m	132.8/6.2	90	284/ 284 – 286	[54]

Continued of Table 5.

Entry	Aldehyde	product	TON/TOF	Yield (%)	m.p. (°C) Obs./Lit.	Ref.
14	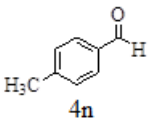 4n	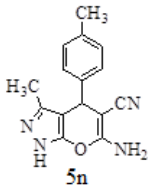 5n	130.7/9.2	87	210/ 208 – 210	[54]
15	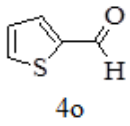 4o	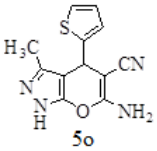 5o	131.4/8.9	84	190/ 190 – 192	[54]
16	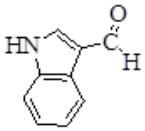 4p	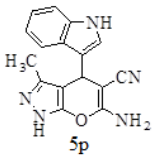 5p	132.9/10.1	86	241 240 – 242	[54]

Michael addition with arylidene malononitrile (4a) gave intermediate (4b), which subsequently yields H-abstraction, and intramolecular cyclization products (4c & 4d), and finally the target product (5) formed through isomerization (Fig. S16).

3.6 Evaluation of the antioxidant activities

Some of the synthesized compounds were screened for their antioxidant activity using the DPPH radical scavenger method [57], and ascorbic acid (VC) as a reference. The compounds with concentrations ranging from 200 μg/μL – 1000 μg/μL were tested in the assay, and results showed variation of the scavenging activity. Compounds 5a, 5h,

Table 6. Reported catalysts and comparison of the methods with the current protocol for the synthesis of pyrano[2, 3-c]pyrazoles*.

Entry	Catalyst	Catalyst (mg)	Condition	Time (min)	Yield** (%)	Ref.
1	Fe_3O_4@Glu	20	rt/Solvent	15	94	[55]
2	$NiFe_3O_4$	30	EtOH	10	80	[56]
3	MNPs@Cu	40	Solvent free	8	95	[57]
4	$Fe_6(OH)_{18}(H_2O)_6$	25	EtOH	180	78	[57]
5	$AuFe_3O_4$@LCys	30	Solvent free	360	76	[58]
6	Fe_3O_4@SiO_2NH_2	35	DCM	30	73	[59]
7	Fe_3O_4@CS	25	Solvent free	480	60	[60]
8	$CoFe_3O_4$@SO_3H	50	Solvent free	15 – 30	85	[61]
9	$AuFe_3O_4$@GSH	35	EtOH	60 – 80	58	[62]
10	$MnFe_2O_4$@Dox	60	EtOH	120	80	[63]
11	**Fe_3O_4@L-Cys**	**25**	**MW/EtOH**	**6**	**94**	**Present**

* Aryl aldehyde (1 mmole), hydrazine hydrate (1 mmole), malononitrile (1 mmole), ethyl acetoacetate (1 mmole), 25 mg catalysts, microwave irradiation at 300 W.

** The reaction completion was monitored by TLC, the catalyst was separated by a strong magnet, and the product was isolated in yield.

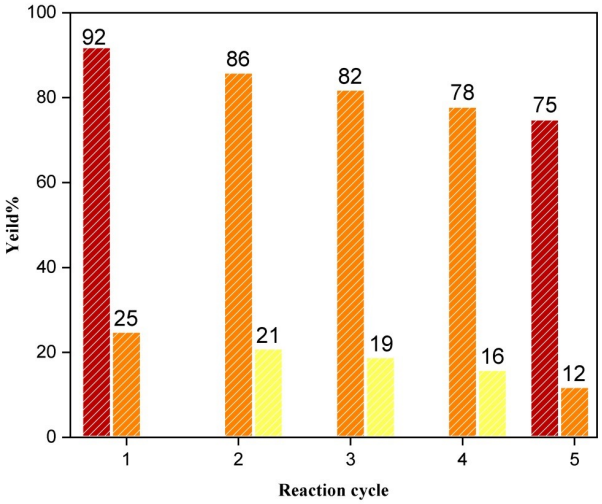

Figure 13. Reusability of the catalysts.

Table 7. Calculation of TON & TOF of the catalysts recycle.

	RUN 1	RUN 2	RUN 3	RUN 3	RUN 4	RUN 5
TON	132.1	130.6	128.1	127.3	125.4	124.8
TOF	8.9	8.8	7.7	6.5	5.6	4.8

and 5i have shown very good scavenging activity, and other compounds **5j**-**5q** have moderate scavenging activity with reference to Fig. 14.

4. Conclusion

MCRs of aromatic aldehyde, malononitrile, hydrazine, and ethyl acetoacetate leading to pyrano[2, 3-c]pyrazoles reported in one-pot catalysed by the heterogeneous catalyst Fe_3O_4@L-Cys. The highlights of this work are the core shell of the catalyst derived from the agro-waste solvent medium, and further surface modification by biopolymer L-Cys, which is non-toxic. The prepared catalyst was characterized using various techniques. The application of this catalyst outlined includes rapid, eco-friendly, recyclable catalyst, inexpensive and simple isolation of the product after recrystallization and avoid use of the chromatographic purification. The synthesized pyrano pyrazole integrity of the product was established by various spectroscopic techniques such as FT-IR, ^{1}H- & ^{13}C-NMR, and LC-MS. Additionally, some of the derivatives demonstrated moderate antioxidant activity when screened for their antioxidant properties (5a, 5h, 5i, 5j, 5k, 5n, 5p, and 5q) against a reference. Overall, the method developed is an efficient, inexpensive, and simple way to isolate a product in a few minutes. The method can be examined further for scale-up reaction synthesis.

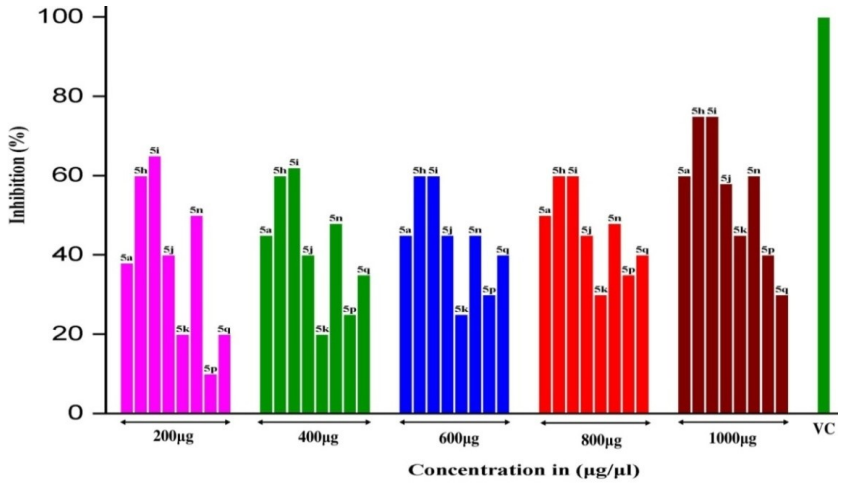

Figure 14. Derivatives of pyrano[2, 3-c]pyrazoles with antioxidant activity.

The method uses greener solvents and is non-toxic to the environment.

Acknowledgement
The authors are thankful to the SERB-SURE, GOI, and RCU-IDR-2022-23 for the financial support to Dr. K.K.

Supplementary information
FT-IR, ^{1}H-, ^{13}C-NMR, and LC-MS of the selected compounds are available in the supplementary.

Authors contributions
Authors have contributed equally in preparing and writing the manuscript.

Availability of data and materials
The data that support the findings of this study are available from the corresponding author, upon reasonable request.

Conflict of interests
The author declare that they have no known competing financial interests or personal relationships that could have appeared to influence the work reported in this paper.

References

[1] D. Y. Lee, H. Li, H. J. Lim, H. J. Lee, R. Jeon, and J. H. Ryu. *J. Med. Food*, **15**(2012):992–999.
DOI: https://doi.org/10.1089/jmf.2012.2275.

[2] H. Lim, K. Kubota, A. Kobayashi, T. Seki, and T. Ariga. *Biosci.Biotech.Biochem.*, **63**(1999):298–301.
DOI: https://doi.org/10.1271/bbb.63.298.

[3] E. Mukwevho, Z. Ferreira, and A. Ayeleso. *Molecules*, **19**(2014): 19376–19389.
DOI: https://doi.org/10.3390/molecules191219376.

[4] M. S. Subramanian, M. S. G. Nandagopal, S. Amin Nordin, K. Thilakavathy, and N. Joseph. *Molecules*, **25**(2020):4111.
DOI: https://doi.org/10.3390/molecules25184111.

[5] I. Fernandez and N. Khiar. *Chem. Rev.*, **103**(2003):3651–3706.
DOI: https://doi.org/10.1021/cr990372u.

[6] K. Khosravi, S. Naserifar, and A. Asgari. *Lett. Org. Chem.*, **13**(2016): 749–756.
DOI: https://doi.org/10.2174/1570178614666161123115100.

[7] A. Padwa, W. H. Bullock, and A. D. Dys zlewski. *J. Org. Chem.*, **55**(1990):955–964.
DOI: https://doi.org/10.1021/jo00290a029.

[8] R. V. Kupwade. *J.Chem.Rev.*, **1**(2019):99–113.
DOI: https://doi.org/10.33945/SAMI/JCR.2019.1.99113.

[9] A. Taketoshi, P. Concepcion, H. Garcia, A. Corma, and M. Haruta. *Bull. Chem. Soc. Jap.*, **86**(2013):1412–1418.
DOI: https://doi.org/10.1246/bcsj.20130075.

[10] M. A. Zolfigol, A. Khazaei, M. Safaiee, M .Mokhlesi, R. Rostamian, M. Bagheri, M. Shiri, and H. G. Kruger. *J. Mole .Catal. A Chem.*, **370**(2013):80–86.
DOI: https://doi.org/10.1016/j.molcata.2012.12.015.

[11] A. Rostami and J. Akradi. *Tetrahedron Lett.*, **51**(2010):3501–3503.
DOI: https://doi.org/10.1016/j.tetlet.2010.04.103.

[12] A. Bravo, B. Dordi, F. Fontana, and F. Minisci. *J. Org. Chem.*, **66**(2001):3232–3234.
DOI: https://doi.org/10.1021/jo0017178.

[13] M. G. Kermanshahi and K. Bahrami. *RSC Adv.*, **9**(2019):36103–36112.
DOI: https://doi.org/10.1039/C9RA06221A.

[14] B. Maleki, S. Hemmati, A. Sedrpoushan, S. S. Ashrafi, and H.Veisi. *RSC. Adv.*, **4**(2014):40505–40510.
DOI: https://doi.org/10.1039/C4RA06132B.

[15] H. Golchoubian and F. Hosse. *Molecules*, **12**(2007):304–311.
DOI: https://doi.org/10.3390/12030304.

[16] M. S. Mashhoori, R. Sandaroos, and A. Z. Moghaddam. *Polycycl. Arom. Compd.*, **42**(2022):5067–5085.
DOI: https://doi.org/10.1080/10406638.2021.1922470.

[17] R. Sandaroos, B. Maleki, S. Naderi, and S. Peiman. *Inorg.Chem.Commun.*, **148**(2023):110294.
DOI: https://doi.org/10.1016/j.inoche.2022.110294.

[18] S. M. Khatami, M. Khalaj, and M. Ghashang. *Iran. J. Catal.*, **13**(2023):475–485.
DOI: https://doi.org/10.30495/ijc.2023.1993331.2039.

[19] M. Dehbashi, M. Aliahmad, M. R. M. Shafiee, and M. Ghashang. *Phosphorus, Sulfur Relat. Elem.*, **188**(2013):864–872.
DOI: https://doi.org/10.1080/10426507.2012.717139.

[20] B. Karimi, M. Ghoreishi-Nezhad, and J. H. Clark. *Org. Lett.*, **7**(2005): 625–628.
DOI: https://doi.org/10.1021/ol047635d.

[21] C. Raj Kumar, B. Thirumalraj, S. M. Chen, P. Veerakumar, and S.-B. Liu. *ACS Appl. Mater. Interfaces*, **9**(2017):31794–31805.
DOI: https://doi.org/10.1021/acsami.7b07645.

[22] B. Karimi and M. Khorasani. *ACS Catal*, **3**(2013):1657–1664.
DOI: https://doi.org/10.1021/cs4003029.

[23] M. Dabiri, H. E. Tavil, N. F. Lehi, S. K. Movahed, A. M. Salmasi, and S. Souri. *J.Phys.Chem.Solids*, **162**(2022):110497.
DOI: https://doi.org/10.1016/j.jpcs.2021.110497.

[24] F. Rajabi, E.Vessally, R. Luque, and L. Voskressen. *sky. Mol. Catal.*, **515**(2021):111931.
DOI: https://doi.org/10.1016/j.mcat.2021.111931.

[25] M. Jin, J. Wang, B. Wang, Z. Guo, and Z. Lv. *Micropor. Mesopor. Mat.*, **277**(2019):84–94.
DOI: https://doi.org/10.1016/j.micromeso.2018.10.021.

[26] A. Sedrpoushan, F. Hosseini-Eshbala, F. Mohanazadeh, and M. Heydari. *Appl. Organomet. Chem.*, **32**(2018):e4004.
DOI: https://doi.org/10.1002/aoc.4004.

[27] S. H. Hosseini, M. Tavakolizadeh, N. Zohreh, and R. Soleyman. *Organomet.Chem.*, **32**(2018):e3953.
DOI: https://doi.org/10.1002/aoc.3953.

[28] N. Zohreh, S. H. Hosseini, A. Pourjavadi, R. Soleyman, and C. Bennett. *J.Indust.Eng.Chem.*, **44**(2016):73–81.
DOI: https://doi.org/10.1016/j.jiec.2016.08.011.

[29] C. M. Tressler, P. Stonehouse, and K. S. Kyler. *Green Chem.*, **18**(2016):4875–4878.
DOI: https://doi.org/10.1039/C6GC00725B.

[30] S. Iraqui, S. S. Kashyap, and M. H. Rashid. *Nanoscal. Adv.*, **2**(2020): 5790–5802.
DOI: https://doi.org/10.1039/D0NA00591F.

[31] L. Sun, R. Zhang, Z. Wang, L. Ju, E. Cao, and Y. Zhang. *J. Mag. Mag. Mater.*, **421**(2017):65–70.
DOI: https://doi.org/10.1016/j.jmmm.2016.08.003.

[32] R. Hajiarab, M. R. M. Shafiee, and M. Ghashang. *Polycycl. Aromat. Compd.*, **43**(2023):2032–2043, .
DOI: https://doi.org/10.1080/10406638.2022.2039231.

[33] R. Hajiarab, M. R. M. Shafiee, and M. Ghashang. *Org. Prep. Proced. Int.*, **54**(2022):259–267, .
DOI: https://doi.org/10.1080/00304948.2022.2033064.

[34] F. Aminsharei, A. Lahijanian, A. Shiehbeigi, S. S. Beiki, and M. Ghashang. *Int. J. Biolog. Macromol.*, **276**(2024):134004.
DOI: https://doi.org/10.1016/j.ijbiomac.2024.134004.

[35] F. Rezaei, H. Alinezhad, and B. Maleki. *Sci Rep*, **13**(2023):20562.
DOI: https://doi.org/10.1038/s41598023-47794-2.

[36] H. Boroum, H. Alinezhad, B. Maleki, and S. Peiman. *Polycyclic Compounds*, **43**(2023):7853–7869.
DOI: https://doi.org/10.1080/10406638.2022.2140683.

[37] R. S. Varma and K. P. Naicker. *Org. Lett.*, **1**(1999):189–191.
DOI: https://doi.org/10.1021/ol990522n.

[38] Q. Wang, W. Ma, Q. Tong, G. Du, J. Wang, M. Zhang, H. Jiang, H. Yang, Y. Liu, and M. Cheng. *Sci. Rep.*, **7**(2017):7209.
DOI: https://doi.org/10.1038/s41598 017-07590-1.

[39] A. Bayat, M. S. Fard, N. Ehyaei, and M. Mahmoodi Hashemi. *RSC Adv.*, **4**(2014):44274–44281.
DOI: https://doi.org/10.1039/C4RA07356H.

[40] Z. Yekke-Ghasemi, M. M. Heravi, M. Malmir, and M. Mirzaei. *Sci. Rep.*, **13**(2023):16752.
DOI: https://doi.org/10.1038/s41598-023-43985-z.

[41] I. A. Al-Masoudi, Y. A. Al-Soud, N. J. Al Salihi, and N. A. Al-Masoudi. *Chem. Het erocycl. Compd.*, **42**(2006):1377–1403.
DOI: https://doi.org/10.1007/s10593-006-0255-3.

[42] M. M. Pearson, D. Rogers, J. D. Cleary, and S. W. Chapman. *An Pharmacotherapy*, **37**(2003):420–432.
DOI: https://doi.org/10.1345/aph.1C261.

[43] N. D. Greer. *Cent., Bayl.*, **20**(2007):188–196.
DOI: https://doi.org/10.1080/08998280.2007.11928283.

[44] I. A. Guralskiy, V. A. Reshetnikov, I. V. Omelchenko, A. Szebesczyk, E. G. Konteckac, and I. O. Fritskya. *J. Mol. Struct.*, **1127**(2017): 164–168.
DOI: https://doi.org/10.1016/j.molstruc.2016.07.094.

[45] Y. L. Fan, X. Ke, and M. Liub. *J. Heterocycle. Chem.*, **55**(2018): 791–802.
DOI: https://doi.org/10.1002/jhet.3112.

[46] M. Onozato, A. Nishigaki, and K. Okoshi. *Poly. Arom. Comp.*, **40**(2018):1291–1301.
DOI: https://doi.org/10.1080/10406638.2018.1540998.

[47] L. Z. Fekri and S. Zeinali. *Appl. Organomet. Chem.*, **17**(2020):20–40.
DOI: https://doi.org/10.1002/aoc.5629.

[48] L. Z. Fekr, K. H. Pour, and S. Zeinali. *J. Organo. chem.*, **915**(2020): 121232–121245.
DOI: https://doi.org/10.1016/j.jorganchem.2020.121232.

[49] M. N. passand, L. Z. Fekri, R. S. Varma, L. Hassanzadi, and F. S. Pashaki. *RSC Adv.*, **12**(2020):834–844.
DOI: https://doi.org/10.1039/D1RA08001F.

[50] A. Bhardwaj. *O. P. P. I.*, **57**(2024):189–217.
DOI: https://doi.org/10.1080/00304948.2024.2431378.

[51] F. S. Ghahfarokhi, A. Ghaemi, and M. R. Kakhki. *Inorg. Nano-Metal. Chem.*, **54**(2023):1179–1186.
DOI: https://doi.org/10.1080/24701556.2023.2166072.

[52] N. Suleymanoglu, R. Ustabas, S. Di, Y. B. Alpasland, and Y. Unvere. *J. Mol. Struct.*, **1150**(2017):82–87.
DOI: https://doi.org/10.1016/j.molstruc.2017.08.075.

[53] R. Kharb, P. C. Sharma, and M. S. Yar. *J. En zyme. Inhib. Med. Chem.*, **16**(2017):1–21.
DOI: https://doi.org/10.3109/14756360903524304.

[54] K. B. Badiger, Giddaerappa, R. Hanumanthappa, L. K. Sannegowda, and K. Kamanna. *Chem. Select.*, **9**(2022):e202104033.
DOI: https://doi.org/10.1002/slct.202104033.

[55] B. M. Chougala, S. Samundeeswari, M. Holiyachi, L. A. Shastri, S. Dodamani, S. Jalalpure, S. R. Dixit, S. D. Joshi, and V. A. Sunagar. *Eur. J. Med. Chem.*, **125**(2017):101–116.
DOI: https://doi.org/10.1016/j.ejmech.2016.09.021.

[56] N. Fu, S. Wang, Y. Zhang, C. Zhang, D. Yang, L. Weng, B. Zhao, and L. Wang. *Eur. J. Med. Chem.*, **136**(2017):596–602.
DOI: https://doi.org/10.1016/j.ejmech.2017.05.001.

[57] K. M. Banu, A. Dinakar, and C. A. narayanan. *Indian J. Pharm. Sci.*, **61**(1999):202–205. URL https://www.ijpsonline.com/articles.

[58] L. Z. Chen, W. W. Sun, L. Bo, J. Q. Wang, C. Xiu, W. J. Tang, J. B. Shi, H. P. Zhou, and X. H. Liu. *Eur. J. Med. Chem.*, **138**(2017): 170–181.
DOI: https://doi.org/10.1016/j.ejmech.2017.06.044.

[59] J. Akhtar, A. A. Khan, Z. Ali, R. Haider, and M. S. Yar. *Eur. J. Med. Chem.*, **125**(2017):143–189.
DOI: https://doi.org/10.1016/j.ejmech.2016.09.023.

[60] R. Gujjar, A. Marwaha, J. White, L. White, S. Creason, D. M. Shackle ford, J. Baldwin, W. N. Charman, S. Buckner, F. S. Charman, P. K. Rathod, , and M. A. Phillips. *J. Med. Chem.*, **52**(2009):1864–1872.
DOI: https://doi.org/10.1021/jm801343r.

[61] Y. Q. Hu, C. Gao, S. Zhang, L. Xu, Z. Xu, L. S. Feng, X. Wu, and F. Zhao. *Eur. J. Med. Chem.*, **139**(2017):22–47.
DOI: https://doi.org/10.1016/j.ejmech.2017.07.061.

[62] A. Duran, H. N. Dogan, and H. Rol las. *Farmaco*, **57**(2002):559–564.
DOI: https://doi.org/10.1016/S0014-827X(02)01248X.

[63] X. Wen, Y. Zhou, J. Zeng, and X. Liu. *Curr. Topics. Med. Chem.*, **20**(2020):1441–1460.
DOI: https://doi.org/10.2174/1568026620666200128143230.